Combining Fast Field Probes with an EMI Detector to reveal Bit Errors induced by ElectroMagnetic Disturbances

Hasan Habib
ESAT-WaveCoRE, M-Group
KU Leuven Bruges Campus
Bruges, Belgium
hasan.habib@kuleuven.be

Tim Claeys
ESAT-WaveCoRE, M-Group
KU Leuven Bruges Campus
Bruges, Belgium
tim.claeys@kuleuven.be

Robert Vogt-Ardatjew
Faculty of Electrical Engineering
University of Twente
Enschede, Netherlands
r.a.vogtardatjew@utwente.nl

Bärbel van den Berg
Medical Technology
MST Hospital
Enschede, Netherlands
b.vandenberg@mst.nl

Guy A. E. Vandenbosch
WaveCoRE
KU Leuven
3001 Leuven, Belgium
guy.vandenbosch@kuleuven.be

Davy Pissoort
ESAT-WaveCoRE, M-Group
KU Leuven Bruges Campus
Bruges, Belgium
davy.pissoort@kuleuven.be

***Abstract*—In this paper, the combination of fast field probes with a previously proposed Electromagnetic Interference (EMI) detector for detecting bit errors in wired communication channels is investigated. This paper studies two EMI detector designs: the Field Probe (FP) EMI detector and the Field Probe Adder Substractor (FPAS) EMI detector. The FP EMI detector solely employs field probes for detection, whereas the FPAS EMI detector uses field probes in addition to the previously proposed A&S EMI detector. The FPAS design overcomes the shortcomings of both the FP EMI detector and the A&S EMI detector by combining their functionality. In order to validate the functionality of the proposed EMI detectors, four distinct PCB-based communication channels are modelled and characterized in the reverberation chamber. These PCB models are intended to represent four types of communication channels. The results show that the proposed FPAS EMI detector can significantly reduce channel false positives in the considered cases.**

***Index Terms*—electromagnetic (EM) resilience, electromagnetic compatibility (EMC), electromagnetic interference (EMI), EMI Risk Management**

I. Introduction

As we are moving toward Industry 4.0, smart cities, and autonomous vehicles, a growing number of electrical/electronic and programmable electronic (E/E/PE) devices are being used in our daily lives. Unfortunately, all E/E/PE devices generate and are also vulnerable to electromagnetic disturbances (EMD) [1]. EMD can affect the performance of the system, and in extreme cases, can cause critical errors [2]. Simultaneously, the increasing demand for safety- and mission-critical systems necessitates a special emphasis on correct and safe operation. For the same reason, combined expertise in the engineering disciplines of Electromagnetic Compatibility (EMC), functional safety, and risk management have gained significant importance. One of the major steps in the development of this field is the IEEE Standard 1848-2020 [3]. This standard focuses on techniques and measurements that can be used to make a system resilient to electromagnetic interference (EMI) by design. These techniques and measures aim to detect errors, faults or malfunctions caused by EMD, correct them if possible such that the system keeps on working (possibly with reduced performance), or is put into a safe state or minimum risk state.

Wired communication channels still play a vital role in modern-day communication systems. Therefore, it is important to focus on their dependability. Many hardware and software-based techniques are designed in order to make a wired communication channel EMI resilient by design. Hardware-based techniques include detection of EMI and frequency, spatial and time diversity [4], [5], [6]. Software-based approaches include Error Detection Codes (EDCs) and Error Correction Codes (ECCs) [7]. The main aim of these techniques and measures is to detect and correct EMI-related bit errors in a communication channel.

A so-called Adder & Subtractor (A&S) EMI detector was proposed in [4]. This aims to detect the EMD induced disturbances in a wired communication channel. This detector is employed at the receiver end and generates a warning when an EMD disturbs the transmitted data. This warning can be used by the system to request a retransmission of the data or shift the system into a safe state. Unfortunately, the A&S EMI detector is not able to detect EMI at EMI frequencies that are an integer multiple of the sampling rate of the detector [4], [8].

Field probes can characterize the electromagnetic (EM) environment and thereby detect the EMD. However, conventional field probes are expensive and slow. In [9],

The research leading to these results has received funding from the European Union's Horizon 2020 research and innovation programme under the Marie Skłodowska-Curie Grant Agreement No 812.790 (MSCA-ETN PETER). This publication reflects only the authors' view, exempting the European Union from any liability. Project website: http://etn-peter.eu/.

[10], Leferink et al. developed cheap, RSSI-based fast probes that can be easily deployed to function as an EMI detector. These probes produce DC output voltages that can be used to measure the field envelope. These probes have a flat frequency response as well as improved sensitivity at low frequencies, allowing them to detect EMI in harsh EM environment [9], [10].

This paper discusses the application of a fast field probe as an EMI detector for a wired communication channel (FP EMI detector) and its limitation in practical applications. Furthermore, the functionality of fast field strength probes and the A&S EMI Detector is combined and discussed in this paper as a new EMI detector (FPAS EMI detector). The primary goal of this approach is to detect EMI in all possible scenarios.

To evaluate the performance of the FP EMI Detector and the FPAS EMI detector, an analysis of the communication channel is conducted in a reverberation room followed by simulations using Python. The performance of the proposed EMI detectors is evaluated using four distinct types of communication channels with varying EMC-aware design. The worst-case coupling, i.e., the highest coupling of the EM field, for each design is measured for the frequency range from 200 MHz to 1 GHz by using a Vector Network Analyser in the reverberation room. Field strength probes are also used near the communication channels to assess the field strength at a specified RF power. Simulations are used to evaluate the response of the EMI detectors for the different communication channels in case of the worst case EMD. The results show that the proposed detectors can be used to detect EMI in a wired communication channel effectively in all tested cases.

Section II of this paper explains the working of the FP EMI detector. This section also explains the fast field probes and different designs of communication channels. Furthermore, this section analyses the performance of the FP EMI detector. In section III the working principles of the FPAS EMI detector is explained, followed by a discussion about the detector's perfomance. Section IV provides concluding remarks.

II. FP EMI Detector

The primary goal of the FP EMI detector implementation in this paper is to detect bit errors in data transmission lines by analysing the EM field strength close to the vulnerable segment of the particular communication channel. If the EM field strength is enough to cause bit errors, a warning is generated. Fig. 1 shows the block diagram of the proposed FP EMI detector.

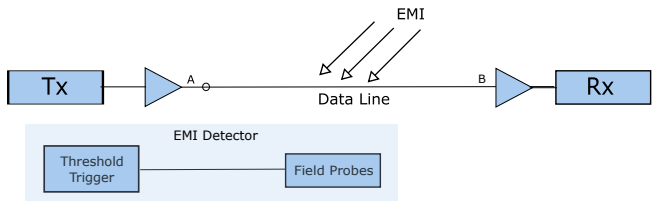

Fig. 1. The FP EMI Detector - Block Diagram

Field probes are commonly used for electric and magnetic field measurements. Traditional probes utilize thermocouples or diode detectors which produce inaccurate measurement results, due to slow response time or quantization error of the analogue-to-digital converter, or their limited dynamic range [11]. Therefore, conventional field probes are not practical to detect fast-changing electric fields, disturbing the data transmission at higher frequencies.

The fast field strength probes, proposed in [9] and [10], can measure rapidly changing electromagnetic fields. They are designed using three orthogonal monopole antennas. These monopole antennas are connected to three logarithmic detectors. The logarithmic detectors have a high dynamic range, and they can monitor an envelope, which can be used to measure peak and RMS values. These properties make them suitable for detecting the field strength generated by high-frequency modern communication systems. They produce a direct current output voltage proportionate to the field strength. These field probes are fast and broadband, making them effective in harsh EM environments.

In the FP EMI detector design, the idea is to use fast field strength probes to analyse the EM field. The threshold trigger can be activated when the field strength is higher than a preset threshold field strength for a particular communication channel.

A. Experimental Setup

Four different communication channels are designed for analysing the performance of the EMI detectors. A reverberation room is used to evaluate the worst-case coupling of the different communication channels and to measure the field strength.

1) Different Communication Channels: The primary goal of these designs is to investigate EM responses to a similar harsh electromagnetic (EM) environment on different communication channels. These are represented by PCB models that correspond to inconsistencies in EMC design guidelines. The top layer of the PCBs uses a pair of microstrip conductors with a 10 cm length and a 2 mm width. They are built with a 50 ohm characteristic impedance. SMA connectors are used to connect microstrip lines to external connections. All PCB designs employ the FR4 substrate and use copper as a conductor. The top side of the PCB designs is shown in Fig.2. The bottom side of the PCB has four different types of ground plane as shown in Fig. 3. The designs can be described as:

- Design 1: In this design, the ground layer is separated into two halves. There is no direct path for return current.
- Design 2: This design employs a cut in the ground level with a 1 cm connection in the corner.
- Design 3: A 5x5 cm hole in a ground plane is exploited in this design to redirect the return current path.
- Design 4: This PCB design satisfies good EMC practices. The full bottom ground layer serves as a return current path.

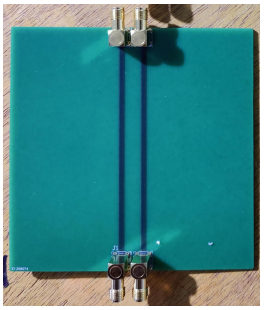

Fig. 2. PCB Designs 1-4, Top View

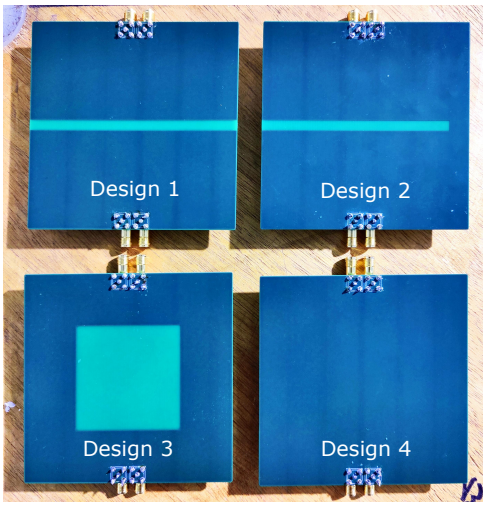

Fig. 3. PCB Designs, Bottom View

2) Measurement Setup: A reverberation room is used to investigate the worst-case coupling to the above-described PCBs. The worst-case coupling to the PCBs is evaluated using a vector network analyser with 501 frequency steps from 200 MHz to 1 GHz. In these measurements, the PCB trace is connected to 50 Ohms of impedance at one end and a vector network analyser at the other. The vector network analyser provides the RF power to the pro-log antenna and also observes the coupled signal on each PCB. Fig. 4 shows the reverberation room setup used for the analysis.

Fig. 4. Reverbration Room Setup

Fig. 5 shows the worst-case coupling (S_{21}) of all four communication channels to the provided RF power. As each communication channel has two lines, the response of each line is analysed separately.

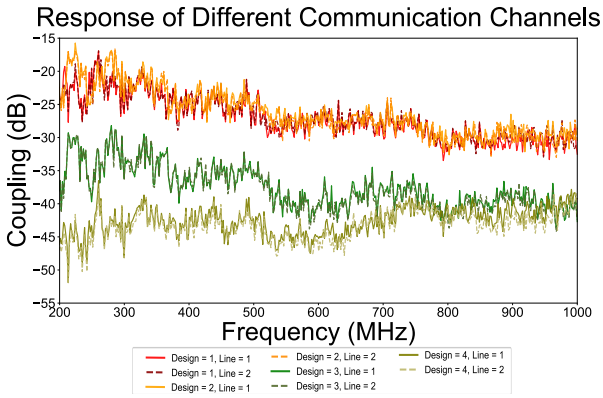

Fig. 5. Response of Different Communication Channels

The average and maximum electric field strength was measured over 100 stirrer positions for each frequency point, for a fixed input power of 15 dBm. In addition, the field strength at the worst-case coupling frequency of each communication channel is also analysed as given in Table I. Fig. 6 shows the maximum and average field strength measured in the reverberation room at the location of the PCBs.

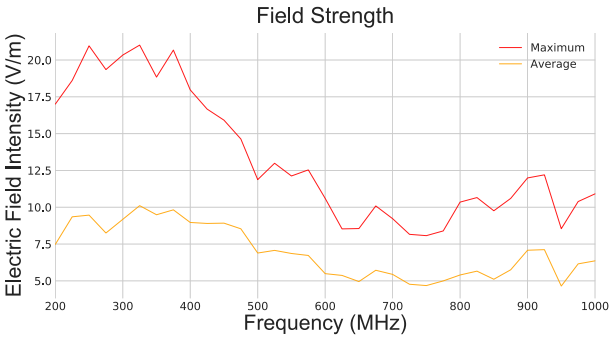

Fig. 6. Electric Field Strength near the Communication Channel @ Input Power = 15 dBm

The field probes produce a wide-bandwidth result, but the coupling is frequency-dependent. Due to this reason, when the exact spectrum is unknown, the maximum of S_{21} is employed as a worst-case scenario in the harsh EM environment. In table I, row 1 to 3 shows the worst-case coupling and frequency measured for each communication channel design. Row 4 of the table provides the field strength, measured at 15 dBm input power for the worst-case coupling frequency.

3) Simulations: To analyse the worst-case response of the FP EMI detector, simulations are performed using Python. In these simulations, 10000 random bits are transmitted through a wired communication channel, and are disturbed by an EM induced voltage. The simulations employs the nonreturn-to-zero-level (NRZ-L) scheme for transmission of

TABLE I
PARAMETERS OF THE FP EMI DETECTOR

	Parameter	Design 1	Design 2	Design 3	Design 4
1	Worst case coupling:				
2	-Frequency	260.2 MHz	224.2 MHz	280 MHz	260.2 MHz
3	-Magnitude	-16.9 dB	-15.73 dB	-28.19 dB	-36.52 dB
4	Field strength (average) at 15dBm RF power	9.0 V/m	9.3 V/m	8.4 V/m	9.0 V/m
5	Bit error can occur:				
6	-RF power (coupled)	-5.65 dBm	-5.65 dBm	-5.65 dBm	-5.65 dBm
7	-Field strength (average)	5.8 V/m	5.3 V/m	20.1 V/m	55.8 V/m
8	A&S Detector fails to detect at:				
9	-RF power (coupled)	10.48 dBm	10.48 dBm	10.48 dBm	10.48 dBm
10	-Field strength (average)	37.3 V/m	33.8 V/m	128.8 V/m	357.1 V/m

bits, using 1V for transmitting '1' and 0V for '0'. At the receiver end, a voltage more than 0.66V is considered as '1' , whereas a value less than 0.33V is considered as '0'. A voltage between 0.33V and 0.66V is regarded as a bit error (worst-case analysis).

The evaluated RF coupled power and field strength that can cause a bit flip are presented in Table I, rows 5-7. In our analysis, the EMD induced voltage of 0.33V can cause a bit flip. Therefore, the RF coupled power for a bit flip is calculated by converting 0.33V to dBm for 50 Ohms impedance. The field strength is evaluated using $E_{\text{Evaluated}} = E_{\text{Measured}} \cdot 10^{\frac{Gain}{20}}$. In this equation, E_{Measured} is the measured field strength and $E_{\text{Evaluated}}$ is the evaluated field strength for a specific frequency. The $Gain$ is the power difference in decibels between the expected coupled power that can cause a bit flip and the coupled power at the measured field strength level. The same calculated field strength threshold is used as a warning trigger for simulations at other frequencies for a specific communication channel.

A sinusoidal EMD induced voltage is used as a disturbance in these simulations. The amplitude of this disturbance is determined by the coupling of each design at a particular frequency. Since the response of both lines of communication channel varies slightly, the line with the worst-case response at a given frequency is considered for the analysis. Also, as the field strength is directly proportional to RF power, it is mathematically calculated for varying RF powers by scaling. The average field strength is used to determine the warning threshold, while the maximum to analyze the worst-case response.

The performance of the FP EMI detector is evaluated for communication channels at different frequencies. Random bits are transmitted at 10 Mbit/s across one of the two data transmission lines, and the EMD induced voltage is used to disrupt the transmitted data based on the worst-case response of the specific design. The simulations for the transmitted bits are repeated by altering the incoming phase of the sinusoidal EMD from 0 to 359 degrees with 10000 steps.

Since bit errors in data transmission lines are dependent upon the EMD induced voltage as well as the voltage of transmitted data, a Signal-to-Interference (SIR) is used. This is defined as

$$\text{SIR} = 20 \cdot \log_{10}\left(\frac{V_{\text{BIT}}^{\text{RMS}}}{V_{\text{EMI}}^{\text{RMS}}}\right) \quad (1)$$

4) Results and Analysis: The performance of the EMI detector is evaluated using the performance assessment definitions given in [12]. These conditions are explained in Table II. The simulations below also use the same color as shown in the Table II.

TABLE II
CONDITIONS FOR ANALYSING AN EMI DETECTOR

Category	Output determined by	Detection	Received value
Data True Positive (DTP)	Data	Correct	Correct
Channel True Positive (CTP)	Channel	Correct	Wrong
Data True Negative (DTN)	Data	Correct	Correct
Channel True Negative (CTN)	Channel	Correct	Wrong
Data False Positive (DFP)	Data	Wrong	Correct
Channel False Positive (CFP)	Channel	Wrong	Wrong
Data False Negative (DFN)	Data	Wrong	Correct
Channel False Negative (CFN)	Channel	Wrong	Wrong

Figs. 7 and 8 shows the response of the communication channel design 2 at 225 MHz and 600 MHz for the FP EMI detector. The field strength of 5.27 V/m is used as the threshold level for all frequencies. It can be observed that although the EMI detector can detect bit errors in all considered cases, it is generating a large number of DFPs at 600 MHz, compromising availability. Indeed, a DFP means that the FP EMI detector warns the system that a bit error could occur, but actually no bit error really occured.

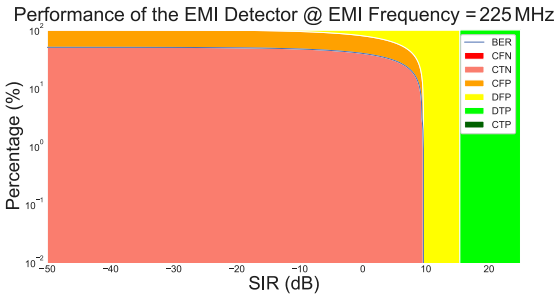

Fig. 7. Response of the FP EMI Detector for Design 2

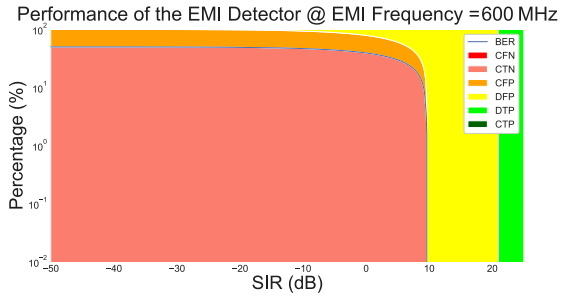

Fig. 8. Response of the FP EMI Detector for Design 2

Similarly, an analysis is performed for communication channel design 3 at 575 MHz, and it can be observed that the FP EMI detector can correctly detect all bit errors as shown in Fig. 9. On the other hand, the EMI detector generates DFPs across a wide range of SIR, again compromising the availability.

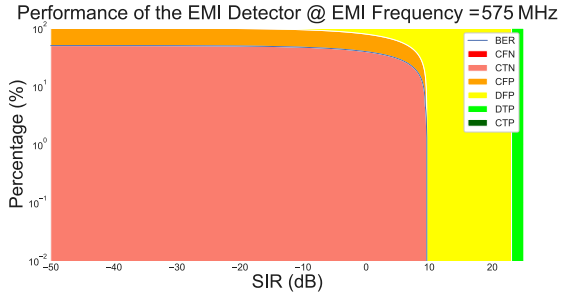

Fig. 9. Response of the FP EMI Detector for Design 3

III. FPAS EMI Detector

The results of the FP EMI detector show that it generates a large number of DFPs. To overcome this limitation, the FPAS EMI detector is proposed. The limitations of the FP EMI detector are addressed by combining it with the A&S EMI detector proposed in [4].

A. The A&S EMI Detector

The A&S EMI detector uses a pair of data transmission lines. The second data transmission line transmits the inverted data. The A&S EMI detector receives the signal from the receiver end of both data transmission lines. It separately adds, and subtracts the signal from both lines, removes the DC constant voltage, and rectifies the output. If the outcome of the adder and/or subtractor is greater than a preset threshold voltage, the A&S EMI detector generates a warning. Fig 10 shows the block diagram of the A&S EMI detector.

Unfortunately, the EMI detector is not able to detect a possible interference when the frequency ratio is an integer multiple of the sampling rate [4]. The frequency ratio is defined as the ratio of the EMI frequency to the bit frequency. Fig. 11 shows the response of the A&S EMI detector when the frequency ratio is 30 and the sampling rate is 3. For this simulation, 10000 random bits are transmitted, and the incoming phase of the EMD-induced voltage is varied from

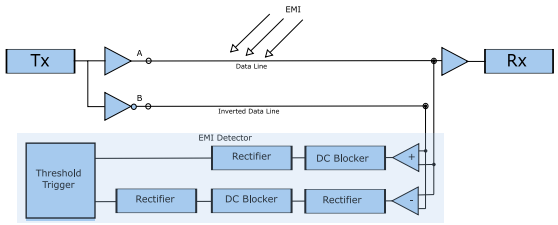

Fig. 10. The A&S EMI Detector - Block Diagram

0 to 359 degrees in 10000 steps. The phase difference of the EMD induced voltage between data transmission lines is set at 45 degrees. The threshold voltage for the A&S EMI detector is 0.33V. The results show that the A&S EMI detector generates CFNs for some values of the SIR.

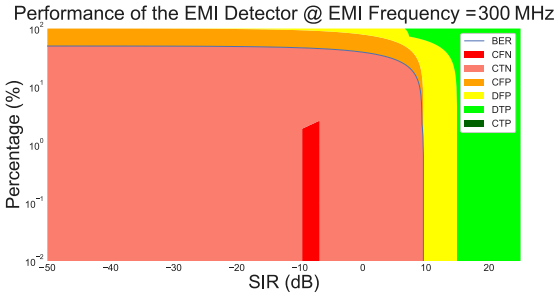

Fig. 11. Response of the A&S EMI Detector for Design 1 @ 300 MHz. Phase difference between two lines = 45°

B. Design of the FPAS EMI Detector

The FPAS EMI detector uses field probes as well as the adder and the subtractor block of the A&S EMI detector to generate a warning. Fig. 12 shows the block diagram of the FPAS EMI detector. The threshold field strength for the FPAS EMI detector is determined by using the worst-case scenario of a particular design covering the SIR values for which the A&S EMI detector starts generating CFNs. To determine the threshold field strength, the phase difference of the EMD induced voltage between the two data transmission lines is set to 45 degrees, the frequency ratio is 30, and the sampling rate is 3. The phase difference of 45 degrees is chosen because, in order to generate CFNs for smaller phase differences, the A&S EMI detector requires a lower SIR value, which corresponds to a higher field strength. Table I, rows 8 to 10 provide the computed coupled power for each design, where the A&S EMI detector starts generating CFNs and the evaluated field strengths at those power levels. The same field strength for a specific design is used as the threshold level of the FPAS EMI detector. The FPAS EMI detector will start generating the warning when the field strength is greater than the determined threshold level for a particular communication channel or the voltage threshold for the A&S detector part is greater than 0.33V.

C. Results

The simulations are performed for the FPAS EMI detector by using a bit frequency of 10 MHz. Figs. 13, 14 and 15 show

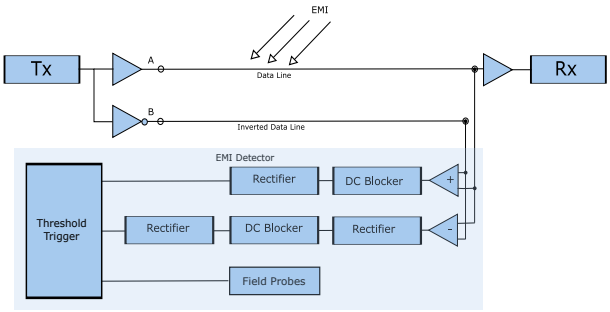

Fig. 12. The FPAS EMI Detector - Block Diagram

the response of the FPAS EMI detector for the communication channels 1, 2 and 4 at different frequencies. These frequencies are selected based on variation in coupling (average, minimum, maximum) compared to the worst-case coupling. The results show that the FPAS EMI detector appropriately generates a warning in all investigated scenarios. Due to the lower number of DFPs, the FPAS EMI detector compromises availability less compared to the FP EMI detector.

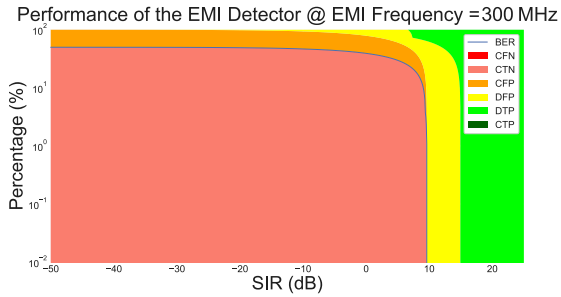

Fig. 13. Response of the FPAS EMI Detector for Design 1

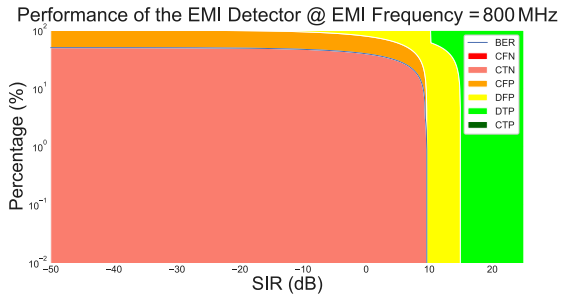

Fig. 14. Response of the FPAS EMI Detector for Design 2

IV. Conclusion and the Future Work

This paper shows the design of the FP EMI detector and the FPAS EMI detector. Both designs of the proposed EMI detector effectively detect bit errors due to EMI for all tested scenarios. However, the FP EMI detector generates a large number of DFPs in some cases, compromising the availability. The FPAS EMI detector overcomes this limitation by using the A&S EMI detector along with the FP EMI detector. However, the FPAS EMI detector continues to produce a limited number of DFPs.

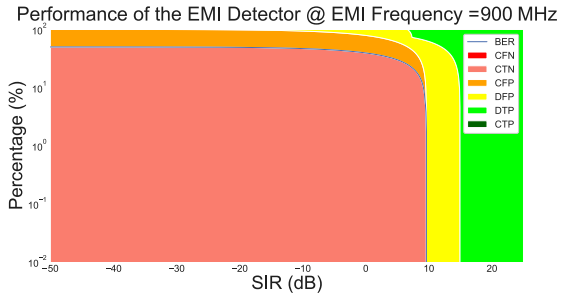

Fig. 15. Response of the FPAS EMI Detector for Design 4

Further studies are needed to determine the placement of fast field probes in real scenarios. It is also important to analyse how the proposed EMI detectors work in a real harsh EM environment. Studies are also needed to further reduce the DFPs.

References

[1] K. Armstrong, "How to manage risks with regard to electromagnetic disturbances," in *IEEE International Symposium on Electromagnetic Compatibility (EMC)*, 2016, pp. 72-77.

[2] K. Armstrong, and A. Duffy, "Reducing the functional safety risks (and other risks) that can be caused by EMI - New IEEE Standard 1848," in *IEEE Letters on Electromagnetic Compatibility Practice and Applications*, vol. 2, no. 3, pp. 53–61, Sept. 2020.

[3] IEEE 1848-2020 - "IEEE techniques & measures to manage functional safety and other risks with regard to electromagnetic disturbances." [Online]. Available: https://standards.ieee.org/standard/1848-2020.html

[4] H. Habib, T. Claeys, D. Vanoost, and G. A. E. Vandenbosch, and D. Pissoort, "Development of an EMI detector based on an inverted data pair with reduced number of false negatives," in *2020 International Symposium on Electromagnetic Compatibility - (EMC EUROPE)*, 2020.

[5] H. Habib, T. Claeys, J. Lannoo, D. Vanoost, G. A. Vandenbosch, and D. Pissoort, "Implementation of Inverted-Pair EMI Detector using a Monte-Carlo Based Simulation Framework," in *2020 29th International Scientific Conference Electronics, ET 2020 - Proceedings*. Institute of Electrical and Electronics Engineers Inc., Sept 2020.

[6] A. Degraeve and D. Pissoort, "Study of the effectiveness of spatially EM-diverse redundant systems under reverberation room conditions," in *IEEE International Symposium on Electromagnetic Compatibility*, vol. 2016-September. Institute of Electrical and Electronics Engineers Inc., Sept 2016, pp. 374–378.

[7] J. Van Waes, J. Lannoo, J. Vankeirsbilck, A. Degraeve, J. Peuteman, D. Vanoost, D. Pissoort, and J. Boydens, "Effectiveness of hamming single error correction codes under harsh electromagnetic disturbances," in *IEEE International Symposium on Electromagnetic Compatibility*, vol. 2018-August. Institute of Electrical and Electronics Engineers Inc., Oct 2018, pp. 271–276.

[8] H. Habib, T. Claeys, R. Perdriau, and D. Pissoort, "Digital and analogue hardware design of an on-board EMI detector," in *2021 13th International Workshop on the Electromagnetic Compatibility of Integrated Circuits (EMC Compo)*, 2022.

[9] F. Leferink, "Fast, broadband, and high-dynamic range 3-d field strength probe," *IEEE Transactions on Electromagnetic Compatibility*, vol. 55, no. 6, pp. 1015–1021, 2013.

[10] F. Leferink and R. Serra, "Fast electromagnetic field strength probes," in *2013 International Symposium on Electromagnetic Compatibility*, 2013, pp. 99–103.

[11] R. Vogt-Ardatjew, R. Serra, L. G. Hiltz, and F. Leferink, "Response time of electromagnetic field strength probes," in *2013 Asia-Pacific Symposium on Electromagnetic Compatibility (APEMC)*, 2013, pp. 1–6.

[12] T. Claeys, H. Tirmizi, H. Habib, D. Vanoost, and G. A. E. Vandenbosch, and D. Pissoort, "A system's perspective on the use of EMI detection and correction methods in safety critical detector," in *2021 International Symposium on Electromagnetic Compatibility - (EMC EUROPE)*, 2021.